Relationship between crystal chemistry and the local structure and electronic properties of $Tl_2Ba_2Ca_2Cu_3O_{10}$ superconductors determined by scanning tunneling microscopy and spectroscopy

Zhe Zhang, Chia-Chun Chen, and Charles M. Lieber*
Department of Chemistry and Division of Applied Sciences, Harvard University, Cambridge, Massachusetts 02138

Bruno Morosin, David S. Ginley, and Eugene L. Venturini
Sandia National Laboratories, Albuquerque, New Mexico 87185
(Received 12 August 1991)

Scanning tunneling microscopy (STM) and scanning tunneling spectroscopy (STS) have been used to characterize the local structure and electronic properties of $Tl_2Ba_2Ca_2Cu_3O_{10}$ single crystals prepared from 4:1:3:6 and 4:1:3:10 stoichiometry melts. Magnetic-susceptibility, resistivity, x-ray-fluorescence, and x-ray-diffraction measurements indicate that samples prepared from the 4:1:3:6 melts (type 1) have a chemical inhomogeneity, while crystals obtained from the 4:1:3:10 melts (type 2) are high quality. STM studies of the type-1 crystals demonstrate that the inhomogeneities can be associated with distortions in the TlO layer atomic structure. STS measurements on the distorted TlO layer of the type-1 samples have shown that this layer is also metallic. STM and STS investigations of the type-2 samples have shown, however, that the TlO layer in these crystals is tetragonal and semiconducting. In addition, a superstructure that is localized over small regions of the TlO surface has been characterized in the type-1 crystals. These results demonstrate that single crystals of the same average structure and composition can exhibit substantial differences in the local-structure electronic states and superconducting properties.

I. INTRODUCTION

The Tl-based superconductors are a structurally and chemically rich class of materials consisting of at least two distinct structural families (Fig. 1).[1-4] A key feature distinguishing these two families is the number of TlO layers, which can be either one or two, in the repeat unit. Additionally, within either family it is possible to have a variable number of copper oxide layers as defined by the basic structural formulas $Tl_2Ba_2Ca_{n-1}Cu_nO_{2n+4}$ and $TlBa_2Ca_{n-1}Cu_nO_{2n+3}$. The variety of different superconducting materials defined by these formulas are readily obtained from quaternary mixtures of the metal oxides, although the conditions needed to obtain pure single-phase crystals that are essential for physical studies and the role that different synthetic methods play in determining the key properties such as the transition temperature (T_c) and the critical current density (J_c) are not well understood.

The highest documented T_c in the thallium-based materials was obtained for $Tl_2Ba_2Ca_2Cu_3O_{10}$ (Tl-2:2:2:3) and is 125 K.[5-7] The transition temperatures reported for the "best" single crystals of Tl-2:2:2:3 have, however, ranged from 108 to 125 K.[7-10] These latter results indicate that subtle features of the crystal chemistry play an important but as yet undetermined role in controlling the superconducting properties of this system. Diffraction studies of these materials have shown that the average structure of the $Tl_2Ba_2Ca_{n-1}Cu_nO_{2n+4}$ materials is tetragonal ($I4/mmm$ space group) with $a=3.855$ Å and $c=35.8$ Å for Tl-2:2:2:3.[7,8,11-13] The microstructure of these materials is, however, believed to be considerably more complex as indicated by the proposed thallium and oxygen positional disorder, oxygen vacancies, and cationic substitution at the Ca and Tl sites.[7,13-17] Despite the considerable effort placed on the Tl-based superconductors, there are few reports that address the relationship between the crystal chemistry and intrinsic structural and electronic properties of these materials,[18-20] although it is essential to understand such factors to properly interpret physical measurements. In this paper we use scanning tunneling microscopy and spectroscopy (STM and STS)

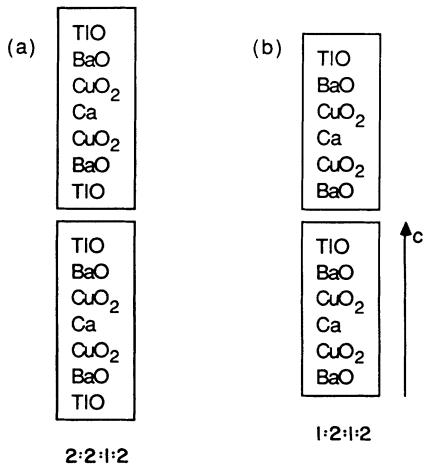

FIG. 1. Schematic views of (a) $n=2$ $Tl_2Ba_2Ca_{n-1}Cu_nO_{2n+4}$ and (b) $n=2$ $TlBa_2Ca_{n-1}Cu_nO_{2n+3}$ that illustrate the different repeat units in these two families of materials.

to characterize the local structure and electronic properties of Tl-2:2:2:3 single crystals prepared from different stoichiometry melts. Our results show that Tl-2:2:2:3 single crystals which have the same average structure and nominal composition can exhibit substantial differences in local structure, electronic states, and superconducting properties when grown from different stoichiometry melts.

II. EXPERIMENTAL METHODS

The single crystals were grown from a melt composition of 4:1:3:X ([Tl]:[Ba]:[Ca]:[Cu]) made up of high-purity (>99.99%) oxides that were stored and processed in an argon atmosphere drybox. This mixture, sealed in a Pt crucible with a wired-on Pt foil lid, was rapidly heated in a vertical tube furnace under an atmosphere of oxygen to 950 °C. The crucible was maintained at 950 °C for 1 h, cooled to 700 °C over 12.5 h and finally cooled to 25 °C in 5–6 h. Single crystals were mechanically removed from the center of the solidified melt away from the crucible walls. A [Ca]/[Ba] ratio of 3/1 was used because Ca-rich melts produce predominantly Tl-2:2:2:3 phase plates. In this paper we report studies of the crystals obtained from two different melt ratios, 4:1:3:6 and 4:1:3:10.

The samples were characterized by magnetic susceptibility [S.H.E., Superconducting-quantum-interference-device (SQUID) magnetometer], four-probe resistivity, x-ray diffraction, and energy dispersive x-ray-fluorescence spectroscopy (EDS) measurements before the STM and STS experiments were carried out. Static magnetization versus temperature was measured with the applied field parallel to the c axis. EDS was performed on both crystal faces to identify crystals with Tl-2:2:2:3 composition. Each Tl-2:2:2:3 single crystal used in the STM experiments was then examined by x-ray precession photography. The crystals used in this study showed no evidence of Pt impurity from the crucible, and thus the results can be unambiguously attributed to variations in melt stoichiometry. Additional experimental details have been described previously.[8,14,19]

The STM images were obtained with modified commercial and home-built instruments operated in an argon-filled glove box equipped with a purification system that reduced the concentrations of oxygen and water to less than 1 ppm. All of the STS measurements were made with a home-built instrument of conventional design.[21] Reproducible and stable ($\geq$6 h) STM and STS measurements were obtained from *in-situ* cleaved samples; the crystals were oriented with the **a-b** plane perpendicular to the tip. The glove-box environment ($\approx 10^{-3}$-Torr O_2) was used to reduce the possibility of oxygen loss from the surface of the materials that may occur in ultrahigh vacuum. The current (I) versus voltage (V) data were acquired by interrupting the STM feedback loop and then stepping the sample-tip bias voltage while digitally storing the resulting changes in tunneling current. The I-V data shown are the average of 20–40 curves obtained at a selected surface site; these measurements likely represent an average over several atomic positions due to drifts during acquisition. Other experimental details have been discussed elsewhere.[18,22]

III. RESULTS

A. Resistivity and susceptibility

Representative susceptibility and resistivity curves are shown for crystals obtained from 4:1:3:6 and 4:1:3:10 melts in Fig. 2; hereafter, we denote these two samples "type 1" and "type 2," respectively. The susceptibility curves were measured in a magnetic field of 25 Oe parallel to the c axis while cooling the sample. For the type-1 and type-2 crystals the T_c's determined from the magnetic data are 90 and 107 K, respectively, The magnetic data show that in addition to a lower T_c the type-1 samples exhibit a significantly broader transition indicative of structural and/or compositional inhomogeneity. A typical resistivity curve obtained from a type-2 crystal exhibits a sharp transition to the zero-resistance superconducting state at 110 K, while the type-1 (lower Cu ratio) sample shows a broad transition with an onset at 101 K; zero resistance is not reached until 72 K in this type-1 sample [Fig. 2(b)]. The widths of the resistivity transitions are thus consistent with the magnetic measurements made on the type-1 and type-2 samples.

The Tl-2:2:2:3 samples obtained from low and high Cu ratio melts obviously show substantially different magnetic and electrical properties, however, the average composition and structure differ very little from that expected for $Tl_2Ba_2Ca_2Cu_3O_{10}$.[6,7,11–13] Although the EDS results are not sufficiently accurate to determine the absolute concentrations of Tl, Ba, Ca, and Cu in a given crystal, we do find that a comparison of data from two crystals provides reproducible relative concentrations.[23] Significantly, EDS analyses of crystals grown from 4:1:3:6 vs 4:1:3:10 showed that the type-1 crystals contained on

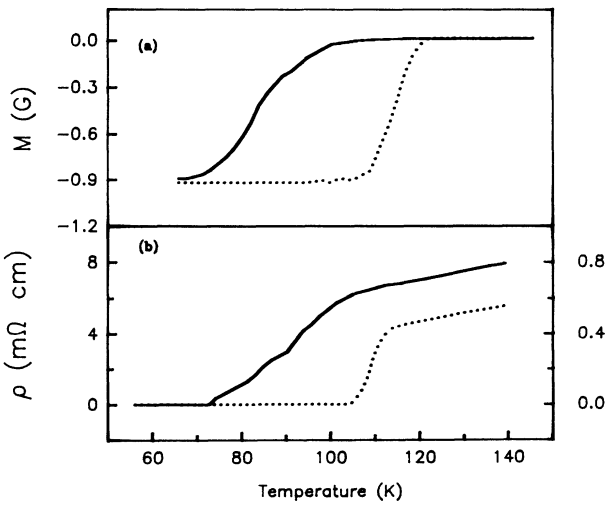

FIG. 2. (a) Magnetization (M) in gauss vs temperature recorded in a field of 25 Oe for type-1 (——) and type-2 (– – – –) samples. (b) Resistivity vs temperature recorded for type-1 (——) and type-2 (– – – –) samples.

average 10 at. % more Tl and 8 at. % less Ba than the type-2 samples.[23] In addition, x-ray precession photography data obtained on crystals from the 4:1:3:6 melt typically exhibit streaking characteristic of a compositional inhomogeneity,[8,23] while precession photographs recorded on type-2 samples show only sharp diffraction spots.

B. Scanning tunneling microscopy

The STM studies were carried out on the type-1 and type-2 crystals that had been characterized as described above. An unfiltered image typical of those obtained on cleaved type-1 samples is shown in Fig. 3; the lattice spacing in this image is 2.4±0.3 Å. The surface structure also has near trigonal symmetry, although the bulk crystal symmetry is tetragonal. Similar images were also obtained for bias voltages between −600 and +600 mV. The 2.4-Å lattice spacing observed in images of the type-1 samples is similar to the average in-plane Tl-O separation reported in x-ray-diffraction studies.[8,11–13] In contrast, the Cu-O separation, 1.93 Å, is significantly shorter, and the Ba-O distance, 2.77 Å, is longer. The ionic BaO layer also does not contribute appreciably to the density of states near the Fermi level and thus is not expected to contribute to the STM tunneling signal. We therefore assign the atomic structure observed in these images to the Tl and O surface sites.

In contrast to the images obtained on the type-1 samples, we find that images obtained on cleaved type-2 Tl-2:2:2:3 crystals exhibit tetragonal atomic structure (Fig. 4). The lattice spacing and angle in this image are 3.6±0.3 Å and 90±5°, respectively. These new features are observed reproducibly in images of cleaved crystals grown from 4:3:1:10 melts (i.e., in samples that exhibit sharp x-ray-diffraction peaks and narrow magnetic and resistive transitions) and thus we believe are intrinsic to the type-2 samples. The observed lattice spacing corresponds well to either the Tl-Tl or O-O bond distances in the TlO layer, and contrasts the appearance of both atomic sites in images of the type-1 samples. Interesting-

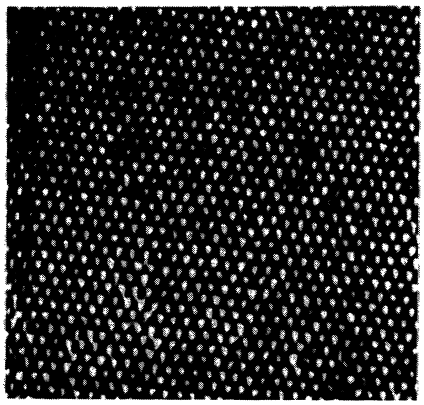

FIG. 3. 80×80 Å^2 gray scale image of a type-1 Tl-2:2:2:3 single crystal recorded with a bias voltage of −260 mV and a tunneling current of 2.1 nA. The image is unfiltered.

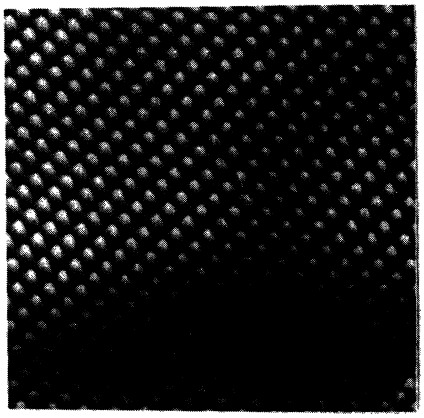

FIG. 4. 80×80 Å^2 perspective view of a Tl-2:2:2:3 type-2 surface recorded with a bias voltage of 410 mV and a tunneling current of 1.2 nA.

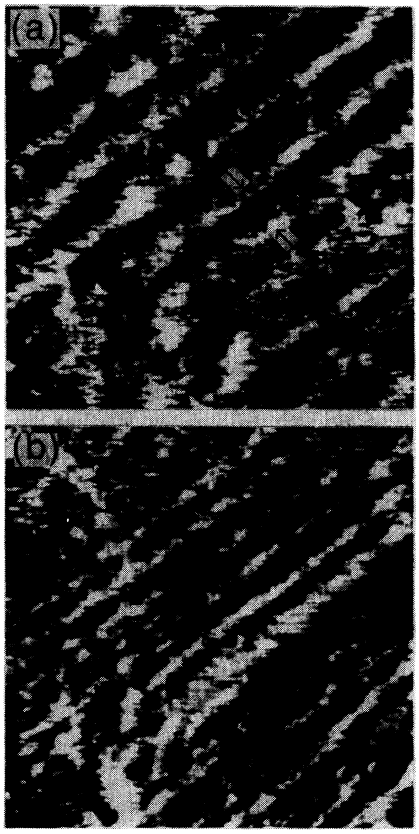

FIG. 5. (a) 200×200 Å^2 image of the one-dimensional superstructure in a type-1 single crystal recorded at bias of −300 mV and tunneling current of 1.1 nA. Two maxima of the superstructure are marked with arrows. The superstructure modulation in this image is ca. 25 Å. (b) 300×300 Å^2 image of the superstructure in another type-1 sample recorded with a bias voltage of 300 mV and a tunneling current of 1.1 nA. The period of the superstructure in this image is irregular. The data in (a) and (b) were low-pass filtered to remove high-frequency noise.

ly, only alternate atomic sites have been observed in STM images of the BiO layer of the structurally related superconductor $Bi_2Sr_2CaCu_2O_8$,[22,24,25] and thus the atomic structure of the TlO layer of type-2 samples appears quite similar to that of the BiO layer in this material.

We have also characterized the surface structure on a larger scale to investigate the possibility of superlattice modulations in the TlO layer. Images of the type-1 samples typically exhibit localized areas that have a one-dimensional superstructure modulation [Figs. 5(a) and 5(b)]. The period of the superstructure in these images varies from 23 to 29 Å but has been observed to vary from 13 to 40 Å in other images. In addition to the variable period, we find that the superstructure is only detected in localized regions $\leq 400 \times 400$ Å^2. The variable nature of the superstructure indicates that it may be due to compositional inhomogeneities. We have not yet observed a superstructure in the images recorded on type-2 samples.

C. Scanning tunneling spectroscopy

To elucidate further the differences between the type-1 and type-2 crystals we have characterized the local electronic structure of these samples by STS. Typical *I-V* curves recorded on the type-1 and type-2 samples are shown in Fig. 6. The feedback stabilized tunneling resistance, 1.3×10^9 Ω, was the same for both of these experiments. In addition, we have plotted the normalized conductivity, $(V/I)dI/dV$, vs V since $(V/I)dI/dV$ provides a measure of the local density of electronic states (DOS) at the surface.[26] The $(V/I)dI/dV$ vs V curves were obtained by numerical differentiation of the *I-V* data. For the type-1 sample the magnitude of the current increases rapidly on either side of $V=0$, while for the type-2 samples we observe reproducibly a finite region near the Fermi level ($V=0$) where the current is much lower. The normalized conductivity curves further highlight the differences between the electronic properties of the two samples. Notably, the $(V/I)dI/dV$ plots show that there is a gap in the DOS for the type-2 samples of ca. 400 meV at the Fermi level while the DOS increases smoothly between ± 1.5 eV for the type-1 samples. Small variations of the *I-V* curves are often observed at different locations of the type-1 and type-2 structural regions, however, these variations are much smaller than the differences shown in Figs. 6(a) and 6(b).

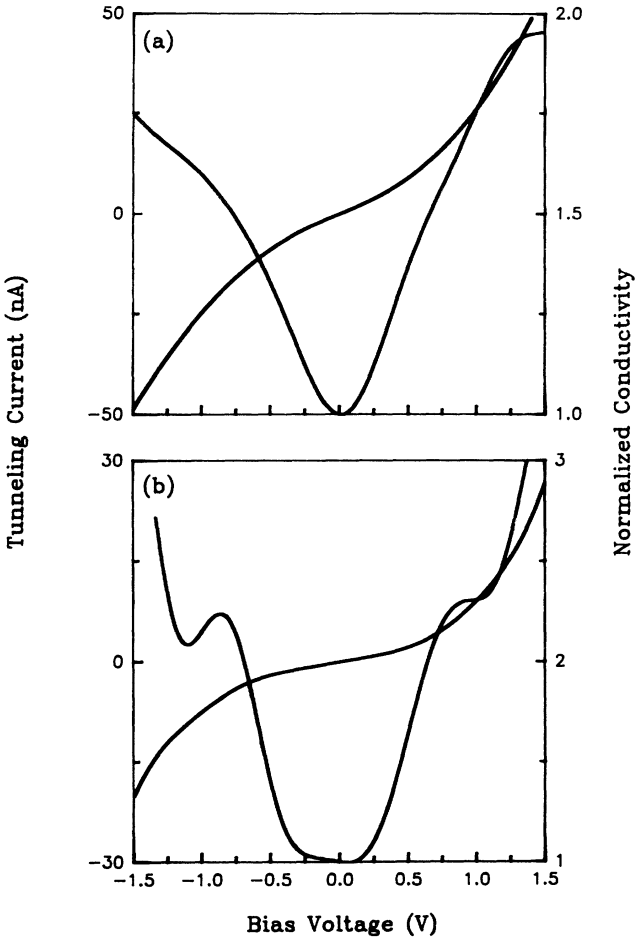

FIG. 6. (a) Current and normalized conductivity, $(V/I)dI/dV$, vs bias voltage curves recorded on a type-1 Tl-2:2:2:3 crystal. (b) Current and normalized conductivity vs voltage curves recorded on a type-2 sample.

IV. DISCUSSION

The widths of the superconducting transitions in the magnetic susceptibility curves [Fig. 2(a)] reflect the quality of the single-crystal samples.[23] Specifically, the susceptibility transition will be broadened by compositional inhomogeneity and magnetic flux pinning. Since field-cooled and zero-field-cooled measurements are reversible above 80 K it is apparent that flux pinning effects are negligible above this temperature. We can thus attribute broadening in the susceptibility transition above 80 K to sample inhomogeneity. The broader transition observed for the type-1 versus type-2 samples thus suggests that crystals grown from the 4:1:3:6 melts have greater compositional inhomogeneity than samples obtained from 4:1:3:10 melts. The widths of the resistivity curves support this interpretation and highlight the high quality of the type-2 samples.

These differences in sample homogeneity are also supported by the EDS and X-ray-diffraction measurements. The EDS data show that crystals obtained from the 4:1:3:6 melt contain more Tl and less Ba than those from the 4:1:3:10 melt, although these results do not provide direct evidence for cation substitution between the TlO and BaO layers. The x-ray precession photographs further demonstrate that while the type-2 samples are relatively homogeneous, the type-1 samples have structural or composition inhomogeneity as evidenced by the streaking of the diffraction spots. Although these conventional measurements (i.e., susceptibility, resistivity, EDS, and x-ray) indicate that the type-1 samples have significantly greater inhomogeneity that the type-2 crystals, they do not identify clearly the atomic level structural and electronic nature of this inhomogeneity. For this

information we turn to the STM and STS results.

The STM images of the type-1 and type-2 samples show two remarkable differences at the atomic scale (Figs. 3 and 4). First, we have found that while the type-1 samples exhibit atomic structure with a period of 2.4 Å the type-2 crystals exhibit structure with a period of ≈ 3.7 Å. As discussed previously the 2.4-Å periodicity is consistent with the average Tl-O spacing determined crystallographically, while the lattice spacing observed for the type-2 samples is consistent with the Tl-Tl or O-O separation.[7,8,11–13] The observation of both Tl and O atomic sites in the type-1 samples shows that both sites contribute comparably to the DOS near the Fermi level, and thus it is reasonable to conclude that the TlO layer in the type-1 samples is metallic. In contrast, the observation of alternate sites in the TlO layer of the type-2 samples indicates that only one site makes a dominant contribution to the tunneling current. A tunneling contribution from only one site (either Tl or O) implies that the TlO layer in the type-2 samples is electronically localized or semiconducting. The STS data directly substantiate these electronic differences in the TlO layers of the type-1 and type-2 samples inferred from the STM images. Results for the type-2 samples [Fig. 6(b)] exhibit a gap in the DOS at the Fermi level which confirms the semiconductorlike electronic nature of this surface. Notably, previous studies have shown that the BiO layer of $Bi_2Sr_2CaCu_2O_8$, which exhibits only alternate atomic sites in STM images, also has a gap in DOS at the Fermi level.[22,25,27] On the other hand, the data for the type-1 samples show no evidence for a gap in the DOS and appear metallic [Fig. 6(a)]. Hence, it is reasonable to associate a metallic TlO layer with the compositionally inhomogeneous type-1 samples and a semiconducting TlO layer with the high-quality type-2 samples.

To understand how the compositional inhomogeneity might cause the difference in electronic properties of the TlO layer in the type-1 and type-2 samples we consider both the lattice symmetry of the STM images and recent theoretical calculations. The type-2 samples, which show every other lattice site, exhibit tetragonal symmetry consistent with the symmetry of the bulk crystal. In contrast, the TlO structure of the type-1 crystals exhibits near trigonal symmetry. It is unlikely that the near trigonal lattice is due to surface adsorption or reconstruction since no such effect is observed in images of the type-2 samples studied under identical conditions. We thus believe that this distortion from the bulk tetragonal crystal symmetry is intrinsic to these samples. Indeed, the diffuse spots observed in the precession photographs of our samples and previous x-ray and neutron-diffraction studies of these materials suggest that the Tl and O sites may be displaced from their ideal lattice sites.[13,15] We thus suggest that the compositional inhomogeneity in the type-1 samples (indicated by susceptibility, resistivity, and EDS measurements) causes the TlO layer to distort from the ideal tetragonal symmetry and thereby become metallic.

The association of the TlO lattice distortions with metallic character is consistent with theoretical calculations. Full-potential linearized-augmented-plane-wave calculations carried out with an undistorted tetragonal TlO layer in Tl-2:2:2:3 and Tl-2:2:1:2 showed that the TlO band contributes very little to the DOS at the Fermi level.[28] On the basis of these results Yu, Massidda, and Freeman suggested that the tetragonal TlO layer was semiconducting. Interestingly, more recent tight-bonding calculations have shown that distortions in the TlO layer structure cause the bottom of the Tl-6*s* band to move below the Fermi level.[29] The distortions thus lead to a metallic TlO layer. In general, our experimental data are consistent with the theoretical calculations where distortions in the TlO layer are essential for making this layer metallic. We note, however, that distortions in our type-1 samples are probably caused by compositional inhomogeneities, which were not considered in the theoretical calculations. Furthermore, the TlO structure of our "best" type-2 samples is tetragonal and undistorted, and thus we suggest that distortions in the TlO layer are deleterious to superconductivity in this system.

Lastly, we briefly consider the one-dimensional superstructure observed in images of the type-1 samples. The fact that the superstructure is not observed uniformly over the entire surface and exhibits several periodicities indicates that this structural modulation is due to compositional inhomogeneities in the type-1 samples. The related superconductor $Bi_2Sr_2CaCu_2O_8$ exhibits a one-dimensional superstructure, although it is observed over the entire BiO layer. In the Bi system it is believed that extra oxygen inserted periodically into the BiO layer may cause this layer to buckle and form the superstructure.[30,31] Hence, we speculate that a compositional inhomogeneity in the type-1 crystals, which has only short-range order, causes the superstructure observed over small regions of the Tl-2:2:2:3 samples. Additional studies of crystals prepared from varying Tl:Ba:Ca:Cu compositions should further elucidate the origin of this interesting structural modulation and its relationship to the periodic superstructure in the Bi-based materials.

V. CONCLUSIONS

In summary, we have used STM and STS to elucidate the local structural and electronic properties of $Tl_2Ba_2Ca_2Cu_3O_{10}$ single crystals prepared from 4:1:3:6 and 4:1:3:10 stoichiometry melts. Conventional magnetic susceptibility, resistivity, EDS, and x-ray-diffraction measurements indicate that single crystals from the 4:1:3:6 melts (type 1) are compositionally inhomogeneous, while crystals obtained from the 4:1:3:10 melts (type 2) are high quality. STM studies of the type-1 crystals demonstrate that the inhomogeneities in these samples distort the TlO layer atomic structure and STS measurements show that this distorted layer is metallic. STM and STS investigations of the type-2 samples show, however, that the TlO layer in these crystals is tetragonal and semiconducting. These data support directly recent theoretical predictions that distortions of the TlO layer lead to metallic behavior, although in our crystals the distortions probably arise from compositional inhomogeneities. In addition, we have suggested that these inhomogeneities in the type-1

crystals cause the superstructure observed over small regions of the TlO surface. Our microscopic studies have thus defined the atomic-level consequences of inhomogeneities in Tl-2:2:2:3 crystals, and furthermore, suggest that STM and STS can be valuable tools in general for elucidating the interplay between the complex physical properties and crystal chemistry in these materials.

ACKNOWLEDGMENTS

C. M. L. acknowledges support from the National Science, David and Lucile Packard, A. P. Sloan, and Camile and Henry Dreyfus Foundations. The work at Sandia National Laboratories was supported, in part, by the Department of Energy Office of Basic Energy Sciences.

*Author to whom correspondence should be addressed.

[1]R. B. Beyers, S. S. P. Parkin, V. Y. Lee, A. I. Nazzal, R. J. Savoy, G. L. Gorman, T. C. Huang, and S. J. La Placa, IBM J. Res. Develop. **33**, 228 (1989).

[2]Z. Z. Sheng and A. M. Hermann, Nature (London) **332**, 55 (1988); **332**, 138 (1988).

[3]M. Hervieu, A. Maigan, C. Martin, C. Michel, J. Provost, and B. Raveau, J. Solid State Chem. **75**, 212 (1988); S. S. P. Parkin, V. Y. Lee, A. I. Nazzal, R. Savoy, R. Beyers, and S. J. La Placa, Phys. Rev. Lett. **61**, 750 (1988); M. A. Subramanian, C. C. Torardi, J. Gopalakrishnan, P. L. Gai, J. C. Calabrese, T. R. Askew, R. B. Flippen, and A. W. Sleight, Science (Washington) **242**, 249 (1988).

[4]H. Ihara, R. Sugise, M. Hirabayashi, N. Terada, M. Jo, K. Hayashi, A. Negishi, M. Tokumoto, Y. Kimura, and T. Shimomura, Nature (London) **334**, 510 (1988); P. Haldar, K. Chen, B. Maheswaran, A. Roig-Janicki, N. K. Jaggi, R. S. Markiewicz, and B. C. Giessen, Science (Washington) **241**, 1198 (1988).

[5]S. S. P. Parkin, V. Y. Lee, E. M. Engler, A. I. Nazzal, T. C. Huang, G. Gorman, R. Savoy, and R. Beyers, Phys. Rev. Lett. **60**, 2539 (1988).

[6]D. S. Ginley, E. L. Venturini, J. F. Kwak, R. J. Baughman, M. J. Carr, P. F. Hlava, J. E. Schirber, and B. Morosin, Physica C **152**, 217 (1988).

[7]C. C. Torardi, M. A. Subramanian, J. C. Calabrese, J. Gopalakrishnan, K. J. Morrissey, T. R. Askew, R. B. Flippen, U. Chowdhry, and A. W. Sleight, Science (Washington) **246**, 631 (1988).

[8]B. Morosin, D. S. Ginley, P. F. Hlava, M. J. Carr, R. J. Baughman, J. E. Schirber, E. L. Venturini, and J. F. Kwak, Physica C **152**, 413 (1988). E. L. Venturini, B. Morosin, D. S. Ginley, P. F. Hlava, M. J. Carr, R. J. Baughman, J. E. Schirber, and J. F. Kwak, in *High Temperature Superconductors: Relationships Between Properties, Structure, and Solid State Chemistry,* edited by J. D. Jorgensen, K. Kitazawa, J. M. Tarascon, M. S. Thompson, and J. B. Torrance, MRS Symposia Proceedings No. 156 (Materials Research Society, Pittsburgh, 1989), p. 239.

[9]H. Takei, T. Kotani, and T. Kateno, Jpn. J. Appl. Phys. **27**, 1378 (1989).

[10]M. A. Subramanian, J. C. Calabrese, C. C. Torardi, J. Gopalakrishnan, T. R. Askew, R. B. Flippen, K. J. Morrissey, U. Chowdhry, and A. W. Sleight, Nature (London) **332**, 420 (1988).

[11]M. A. Subramanian, J. B. Parise, J. C. Calabrese, C. C. Torardi, J. Gopalakrishnan, and A. W. Sleight, J. Solid State Chem. **77**, 192 (1988).

[12]R. Beyers, S. S. P. Parkin, V. Y. Lee, A. I. Nazzal, R. Savay, G. Gorman, and T. C. Huang, Appl. Phys. Lett. **53**, 432 (1988).

[13]D. E. Cox, C. C. Torardi, M. A. Subramanian, J. Gopalakrishnan, and A. W. Sleight, Phys. Rev. B **38**, 6624 (1988).

[14]B. Morosin, R. J. Baughman, D. S. Ginley, J. E. Schirber, and E. L. Venturini, Physica C **161**, 115 (1990).

[15]W. Dmowski, B. H. Toby, T. Egami, M. A. Subramanian, J. Gopalakrishnan, and A. W. Sleight, Phys. Rev. Lett. **61**, 2608 (1988); T. Egami, B. H. Toby, W. Dmowski, S. Billinge, P. K. Davies, J. D. Jorgensen, M. A. Subramanian, and A. W. Sleight, Physica C **162**, 93 (1989).

[16]A. Maignan, C. Martin, M. Huve, J. Provost, M. Hervieu, C. Michel, and B. Raveau, Physica C **170**, 350 (1990).

[17]X. L. Wu, C. M. Lieber, D. S. Ginley, and R. J. Baughman, Appl. Phys. Lett. **55**, 2129 (1989).

[18]Z. Zhang, C. M. Lieber, D. S. Ginley, R. J. Baughman, and B. Morosin, J. Vac. Sci. Technol. B **9**, 1009 (1991).

[19]E. L. Venturini, C. P. Tigges, R. J. Baughman, D. S. Ginley, and B. Morosin, in *High-Temperature Superconductors: Fundamental Properties and Novel Materials Processing,* edited by D. Christen, J. Narayan, and L. Schneemeyer, MRS Symposia Proceedings No. 169 (Materials Research Society, Pittsburgh, 1990), p. 1069.; E. L. Venturini, C. P. Tigges, R. J. Baughman, B. Morosin, J. C. Barbour, M. A. Mitchell, and D. S. Ginley, J. Cryst. Growth **109**, 441 (1991).

[20]M. Hervieu, C. Michel, and B. Raveau, Microsc. Microanal. Microstruct. **1**, 327 (1990).

[21]P. Avouris, J. Phys. Chem. **94**, 2246 (1990).

[22]X. L. Wu, Z. Zhang, Y. L. Wang, and C. M. Lieber, Science (Washington) **248**, 1211 (1990).

[23]C. P. Tigges, E. L. Venturini, J. F. Kwak, B. Morosin, R. J. Baughman, and D. S. Ginley, Appl. Phys. Lett. **57**, 517 (1990); B. Morosin, D. S. Ginley, E. L. Venturini, R. J. Baughman, and C. P. Tigges, Physica C **172**, 413 (1991).

[24]M. D. Kirk, J. Nogami, A. A. Baski, D. B. Mitzi, A. Kapitulnik, T. H. Geballe, and C. F. Quate, Science (Washington) **242**, 1673 (1988).

[25]C. K. Shih, R. M. Feenstra, J. R. Kirtley, and G. V. Chandrashekhar, Phys. Rev. B **40**, 2682 (1989); C. K. Shih, R. M. Feenstra, and G. V. Chandrashekhar, *ibid.* **43**, 7913 (1991).

[26]R. M. Feenstra, J. A. Stroscio, and S. P. Fine, Surf. Sci. **181**, 295 (1987).

[27]Z. Zhang, Y. L. Wang, X. L. Wu, J. L. Huang, and C. M. Lieber, Phys. Rev. B **42**, 1082 (1990).

[28]J. Yu, S. Massidda, and A. J. Freeman, Physica C **152**, 273 (1988).

[29]D. Jung, M. H. Whangbo, N. Herron, and C. C. Torardi, Physica C **160**, 381 (1989).

[30]Y. Le Page, W. R. McKinnon, J. -M. Tarascon, and P. Barboux, Phys. Rev. B **40**, 6810 (1989).

[31]H. W. Zandbergen, W. A. Groen, F. C. Mijlhoff, G. Tendeloo, and S. Amelinckx, Physica C **156**, 325 (1988).

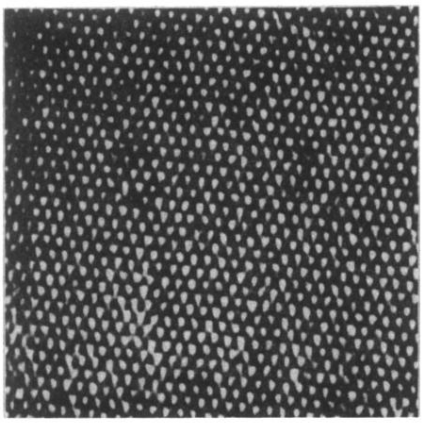

FIG. 3. 80×80 Å^2 gray scale image of a type-1 Tl-2:2:2:3 single crystal recorded with a bias voltage of -260 mV and a tunneling current of 2.1 nA. The image is unfiltered.

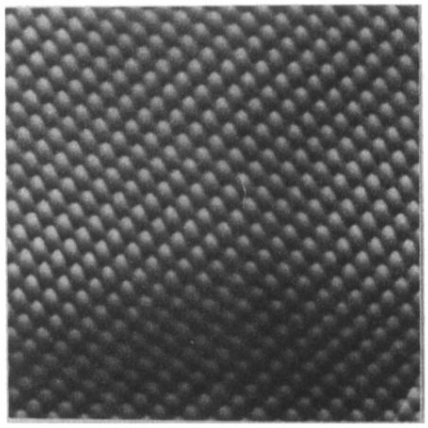

FIG. 4. 80×80 Å^2 perspective view of a Tl-2:2:2:3 type-2 surface recorded with a bias voltage of 410 mV and a tunneling current of 1.2 nA.

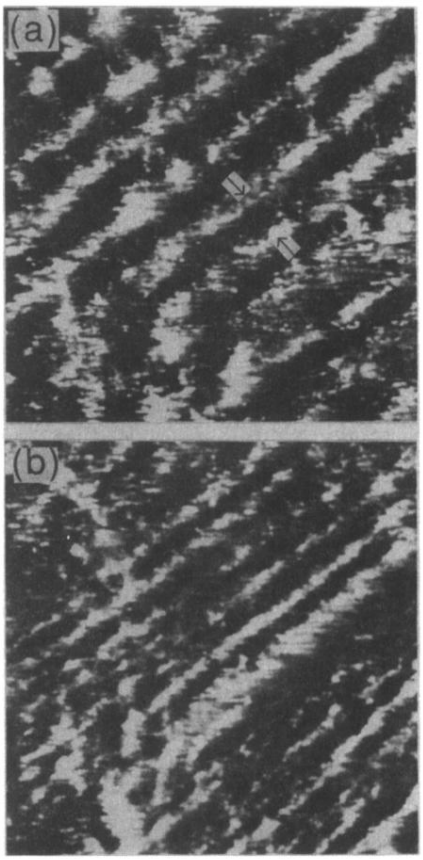

FIG. 5. (a) 200×200 Å^2 image of the one-dimensional superstructure in a type-1 single crystal recorded at bias of -300 mV and tunneling current of 1.1 nA. Two maxima of the superstructure are marked with arrows. The superstructure modulation in this image is ca. 25 Å. (b) 300×300 Å^2 image of the superstructure in another type-1 sample recorded with a bias voltage of 300 mV and a tunneling current of 1.1 nA. The period of the superstructure in this image is irregular. The data in (a) and (b) were low-pass filtered to remove high-frequency noise.